arXiv:1611.00623v1 [astro-ph.HE] 2 Nov 2016

Ultrafast outflows in ultraluminous X-ray sources

Ciro Pinto[1,⋆], **Andy Fabian**[1], **Matthew Middleton**[1,2], and **Dom Walton**[1,3]

[1] Institute of Astronomy, Madingley Rd, Cambridge, CB3 0HA, UK
[2] Physics & Astronomy, University of Southampton, Southampton, Hampshire SO17 1BJ, UK
[3] Jet Propulsion Laboratory, California Institute of Technology, Pasadena, CA 91109, USA

Received November 3, 2016

Key words X-ray binaries: accretion, accretion disks, winds - black hole physics

Ultraluminous X-ray sources (ULXs) are bright extragalactic sources with X-ray luminosities above 10^{39} erg/s powered by accretion onto compact objects. According to the first studies performed with XMM-*Newton* ULXs seemed to be excellent candidates to host intermediate-mass black holes ($10^{2-4} M_{\odot}$). However, in the last years the interpretation of super-Eddington accretion onto stellar-mass black holes or neutron stars for most ULXs has gained a strong consensus. One critical missing piece to confirm the super-Eddington scenario was the direct detection of the massive, radiatively-driven winds expected as atomic emission/absorption lines in ULX spectra. The first evidence for winds was found as residuals in the soft X-ray spectra of ULXs. Most recently we have been able to resolve these residuals into rest-frame emission and blueshifted ($\sim 0.2c$) absorption lines arising from highly ionized gas in the deep high-resolution XMM-*Newton* spectra of two ultraluminous X-ray sources. The compact object is therefore surrounded by powerful ultrafast winds as predicted by models of hyper-Eddington accretion. Here we discuss the relevance of these discoveries and the importance of further, deep, XMM-*Newton* observations of powerful winds in many other ultraluminous X-ray sources to estimate the energetics of the wind, the geometry of the system, and the masses of the central accretors.

© 0000 WILEY-VCH Verlag GmbH & Co. KGaA, Weinheim

1 Introduction

Ultraluminous X-ray sources (ULXs) are extragalactic, off-nucleus, point sources in galaxies and have X-ray luminosities that exceed the Eddington limit for a 10M$_{\odot}$black hole (BH), or 10^{39} erg/s. Early detections of ULXs were possible with the *Einstein* observatory (Long & van Speybroeck 1983). In the last two decades, X-ray surveys have observed hundreds of ULXs with different facilities (ROSAT, Liu & Bregman 2005; *Chandra*, Swartz et al. 2004; XMM-*Newton*, Walton et al. 2011). Two main scenarios have been proposed to describe the nature of these exotic objects, both implying accretion onto compact objects.

One scenario proposes ULXs to be powered by intermediate-mass ($10^{2-4} M_{\odot}$) black holes (IMBHs) accreting in a sub-Eddington regime similar to the well-studied Galactic BHs (e.g., Kaaret et al. 2001; Miller et al. 2003). Probing the census of IMBHs is a crucial ingredient to understand the growth of supermassive black holes (SMBHs) powering active galaxies (Kormendy & Ho 2013). These objects are also the most likely explanation for the far bright end of the ULXs, called hyperluminous X-ray sources, whose prototype is ESO 243-49 HLX-1 (Farrell et al. 2009). Its outburst and spectral states are similar to the sub-Eddington Galactic BHs.

The other scenario describes ULXs as stellar-mass black holes or neutron stars accreting several orders of magnitude above the classic Eddington limit (super-Eddington or super-critical accretion). Super-Eddington accretion can be explained with several models: photon-bubble instability in thin disks (Begelman 2002), inefficient regime of accretion in slim disks (Kawaguchi 2003), and radiation-supported thick disks (Poutanen et al. 2007). Geometrical beaming (King et al. 2001) may provide a further increase of luminosity in the line of sight, although observations rule out extreme beaming in ULXs (e.g., Berghea et al. 2010; Moon et al. 2011). Super-Eddington accretion is another crucial ingredient to understand SMBHs growth because the discovery of fully grown SMBH in early stages of the Universe requires long periods of high accretion (Fan et al. 2003, Volonteri et al. 2013).

ULXs enable both the study of super-Eddington accretion and the search for IMBHs and, therefore, have an important impact on cosmology.

The first masses inferred dynamically from optical data revealed two ULXs to be powered by compact objects with masses in the stellar-mass black hole range (Liu et al. 2013; Motch et al. 2014). The detection of bright radio emission confirmed another stellar-mass compact object in a transient source in M 31 (Middleton et al. 2013). M 82 X-2 shows pulsations, which indicates a neutron star as the accretor (Bachetti et al. 2014). A clear downturn has been detected in most high-quality XMM-*Newton* and NuSTAR ULX spectra at energies of a few keV (e.g. Roberts et al. 2005; Stobbart, Roberts & Wilms 2006; Bachetti et al. 2013; Walton et al. 2014). Most ULX X-ray spectra can therefore be de-

⋆ Corresponding author: e-mail: cpinto@ast.cam.ac.uk

© 0000 WILEY-VCH Verlag GmbH & Co. KGaA, Weinheim

scribed by a combination of a hard component showing this downturn and a soft excess, which is not consistent with the classic sub-Eddington BH accretion states.

In a most recent work, Pinto et al. (2016), we have discovered the presence of rest-frame emission and blueshifted ($0.2c$) absorption lines arising from highly ionized gas in the deep high-resolution XMM-*Newton* spectra of two ultraluminous X-ray sources: NGC 1313 X-1 and NGC 5408 X-1. These features resolved the soft X-ray residuals that were earlier detected in the spectra of these and other ULXs taken with the European Photon Imaging Camera (EPIC, CCD) at moderate resolution (Middleton et al. 2014, 2015). This discovery was further strengthened by a follow up paper in which we detected its highly energetic Fe K counterpart in the long-exposure XMM-*Newton* CCD and NuSTAR CdZnTe spectra (Walton et al. 2016). The discovery of the long sought powerful winds in ULXs provides further support to the scenario of super-Eddington accretion and in this paper we discuss the relevance of these discoveries and the importance of further, deep, XMM-*Newton* observations of powerful winds in many other ultraluminous X-ray sources in order to estimate the energetics of the wind, the geometry of the system, and the black hole masses.

2 Soft X-ray spectral features of ULXs

It has been known for a decade that soft ULXs show residuals to their continuum spectral fits (e.g. Stobbart et al. 2006). It was not clear whether they were produced by the hot phase of the interstellar medium of the host galaxies, by gas shocks in the optical nebulae around the ULXs or by the gas accreted onto the compact objects. Middleton et al. (2014) investigated the residuals in the archetypal ULXs NGC 5408 X-1 and NGC 6946 X-1, and found that they can be explained as broad absorption lines from a partially ionised and blueshifted ($v \sim 0.1c$) medium in agreement with absorption from the optically thin phase of a turbulent outflowing wind, located outside the last scattering surface of the optically-thick region. Sutton, Roberts, & Middleton (2015) used *Chandra* high spatial-resolution spectra of NGC 5408 X-1 to show that the residuals were mostly associated with the ULX itself rather than to star formation or hot gas in the host galaxy.

2.1 The shape of the spectral residuals

In a crucial step towards the understanding of the spectral residuals we show that their shape is similar among six different ULXs with high quality soft X-ray spectra (Middleton et al. 2015, see also Fig. 1), which suggests that they have the same origin. We have further probed the relation between the residuals and the spectral states of NGC 1313 X-1, which has the largest dynamical range in its hardness of any of the ULXs with detectable residuals. A clear anti-correlation between spectral hardness (ratio between the flux in the 1–10 keV and the 0.3–1 keV bands) and the strength (or equivalent width) of the features was found (see Fig. 2), which rules out an origin due to reflection on top of the accretion disk (expected to increase with the hardness) or to any galactic / star formation event. This is instead consistent with wind models, where for moderate-to-high inclination angles an increase in accretion rate leads to a stronger wind, which both softens the spectrum and deposits more material into the optically thin medium surrounding the ULX, that deepens the absorption features (e.g., Poutanen et al. 2007).

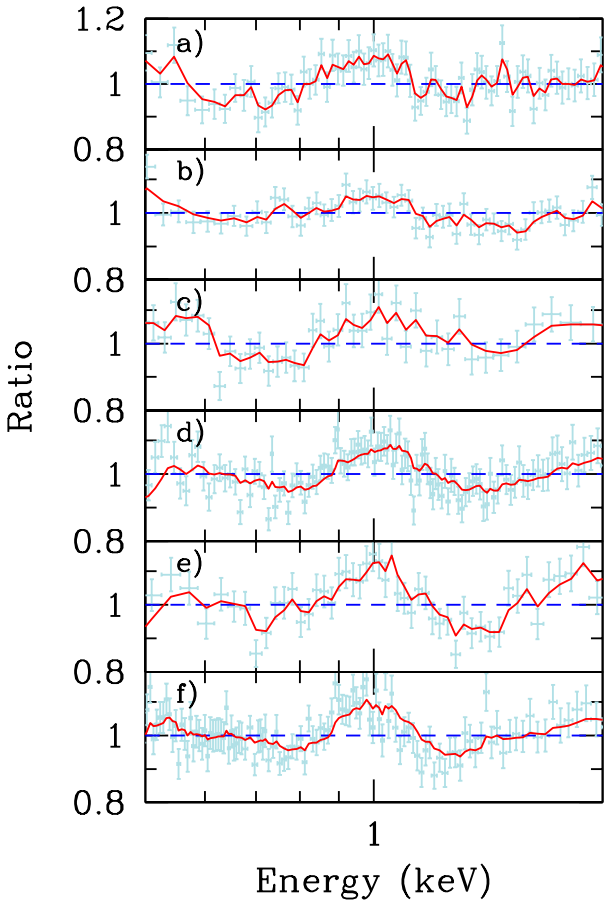

Fig. 1 Soft X-ray residuals to continuum models for 6 ULXs. The objects are: (a) NGC 1313 X-1, (b) Ho IX X-1, (c) Ho II X-1, (d) NGC 55 ULX-1, (e) NGC 6946 X-1, and (f) NGC 5408 X-1. The spectral data are shown in light blue and plotted as a ratio to the best fitting model, and an exponentially smoothed function is plotted in red to highlight the commonality in the shape of the residuals. Figure from Middleton et al. (2015).

2.2 High-resolution X-ray spectroscopy with gratings

The XMM-*Newton* and *Chandra* X-ray satellites are provided with spectrometers that have a high ($E/\Delta E \sim 100-1000$) energy spectral resolution and are, therefore, able to resolved spectral features narrower than $1000\,\mathrm{km\,s^{-1}}$: the gratings (Brinkman et al. 2000, den Herder et al. 2001 and

© 0000 WILEY-VCH Verlag GmbH & Co. KGaA, Weinheim

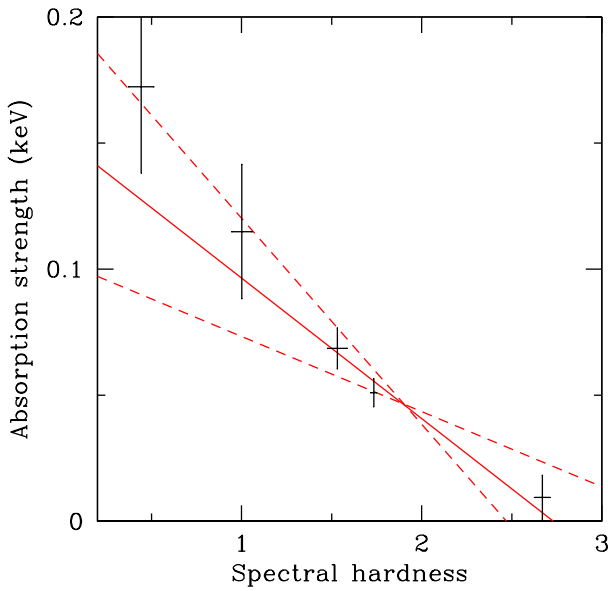

Fig. 2 Absorption strength from the spectral fits plotted against spectral hardness (with 1σ error bars). The solid red line is the best-fitting relation (with a slope of 0.05 ± 0.01) and the dashed lines are the extremal range of relations (from the 3σ errors on the slope and intercept). Figure from Middleton et al. (2015).

Canizares et al. 2005). Despite their high resolution power, the gratings are often ignored because they have much lower effective area than the CCD spectrometers, provide only 1D spectroscopy (along their cross dispersion direction) and require a careful data reduction, particularly for extended and/or multiple sources in the field of view. However, at least for XMM-*Newton*, the reflection grating spectrometers (RGS) work in parallel with the EPIC cameras, and the archive is therefore rich with unexplored high-spectral resolution RGS data. There is a wealth of RGS public observations of ULXs: NGC 1313 X-1 and NGC 5408 X-1, in particular, were observed for several XMM-*Newton* orbits.

2.3 Zooming onto NGC 1313 X-1 and NGC 5408 X-1

NGC 1313 X-1 and NGC 5408 X-1 are two archetypal ULXs showing all the classical properties of the bulk of the population and have X-ray (0.2–10 keV) luminosities up to $\sim 10^{40}$ erg/s. They have been extensively observed in spectral states where a large fraction of their flux emerges below 2 keV (Stobbart et al. 2006; Gladstone et al. 2009) showing strong spectral deviations (0.6–1.2 keV) from the underlying continuum in CCD spectra (see Fig. 1). These two ULXs are within a 5 Mpc distance, are rather isolated, and have the longest set of full XMM-*Newton* orbits. This allows for a comparatively clean, high energy-resolution study of the features seen in CCD spectra.

In Pinto et al. (2016) we collect the three and six full XMM-*Newton* orbits of NGC 1313 X-1 and NGC 5408 X-1, obtaining 345.6 ks and 644.9 ks solar-flared clean data. We stack the spectra of each source with an advanced technique that accounts for the different background subtraction of the two RGS spectrometers. This provided the two best high-resolution X-ray spectra ever taken for ULXs (see Fig.3).

The RGS spectra of NGC 1313 X-1 and NGC 5408 X-1 show a wealth of emission and absorption features including the absorption features produced by the foreground Galactic interstellar medium (see, e.g., Pinto et al. 2013). At first, we could identify strong, rest-frame emission lines from a mixture of elements at varying degrees of ionization, including Ne X ($\lambda = 12.1$ Å), O VIII (19.0 Å), O VII (21.6 Å), and Fe XVII ($15.0, 17.1$ Å). There are several narrow absorption-like features including a broad depression at the blue side ($10 - 12$ Å) of the Ne X emission line in NGC 1313 X-1. These spectral features actually resolve the residuals shown by Middleton et al. (2014, 2015). Before trying to model these emission and absorption features we constrain the spectral continuum by simultaneously fitting the EPIC and RGS spectra of these sources with a standard blackbody plus powerlaw emission model, multiplied by neutral absorption both from our Galaxy and intrinsic to NGC 1313.

We analyze the spectral features using the high-resolution RGS spectra and adopting the combined EPIC–RGS spectral continuum. We first measure their significance by fitting a Gaussian over the 7–27 Å wavelength range with increments of 0.05 Å. We have also tested the effects of adopting different line widths. The strongest emission lines, found at their rest frame wavelengths, are detected at a 3σ level each. The strongest absorption features, e.g. between $10 - 12$ Å in NGC 1313 X-1, are also detected at 3σ, if interpreted as blueshifted Ne IX-X or Fe XVIII absorption (and accounting for the look-elsewhere effect).

2.4 Ultrafast outflows in the ULX grating spectra

We modeled the emission lines with a rest-frame, collisional ionization equilibrium (CIE) plasma, which includes an underlying weak thermal continuum at an average temperature of 0.8 keV ($\sim 10^7$ K; see Fig.3). The absorption lines can be well modelled with a mildly ionized ($\log \xi = 2.25 \pm 0.05$ or $\xi \sim 180\,\mathrm{erg\,cm\,s^{-1}}$) absorbing gas in photoionization equilibrium applied to the continuum. This absorber has a tremendous outflow velocity of ~ 0.2 times the speed of light. The inclusion of a rest-frame absorber with the same ionization parameter provides a slight improvement to the fit. These model adopts the same line width for absorption and emission lines ($< 500\,\mathrm{km\,s^{-1}}$). The large depression between $10-12$ Å in NGC 1313 X-1 can also be modeled with an absorption with higher ($\log \xi = 4.5$) ionization parameter and relativistic ($\sim 0.1c$) line broadening (see blue line in Fig.3, top left panel). NGC 5408 X-1 also shows sharp emission features similar to those detected in NGC 1313 X-1, but the outflow seems to be more structured with the emission lines being stronger than the absorption features. A better fit is obtained with a multiphase emission (CIE) and absorption (Xabs) model (see blue line in Fig.3, top right panel). This could suggest a different geometry or view angle for

© 0000 WILEY-VCH Verlag GmbH & Co. KGaA, Weinheim

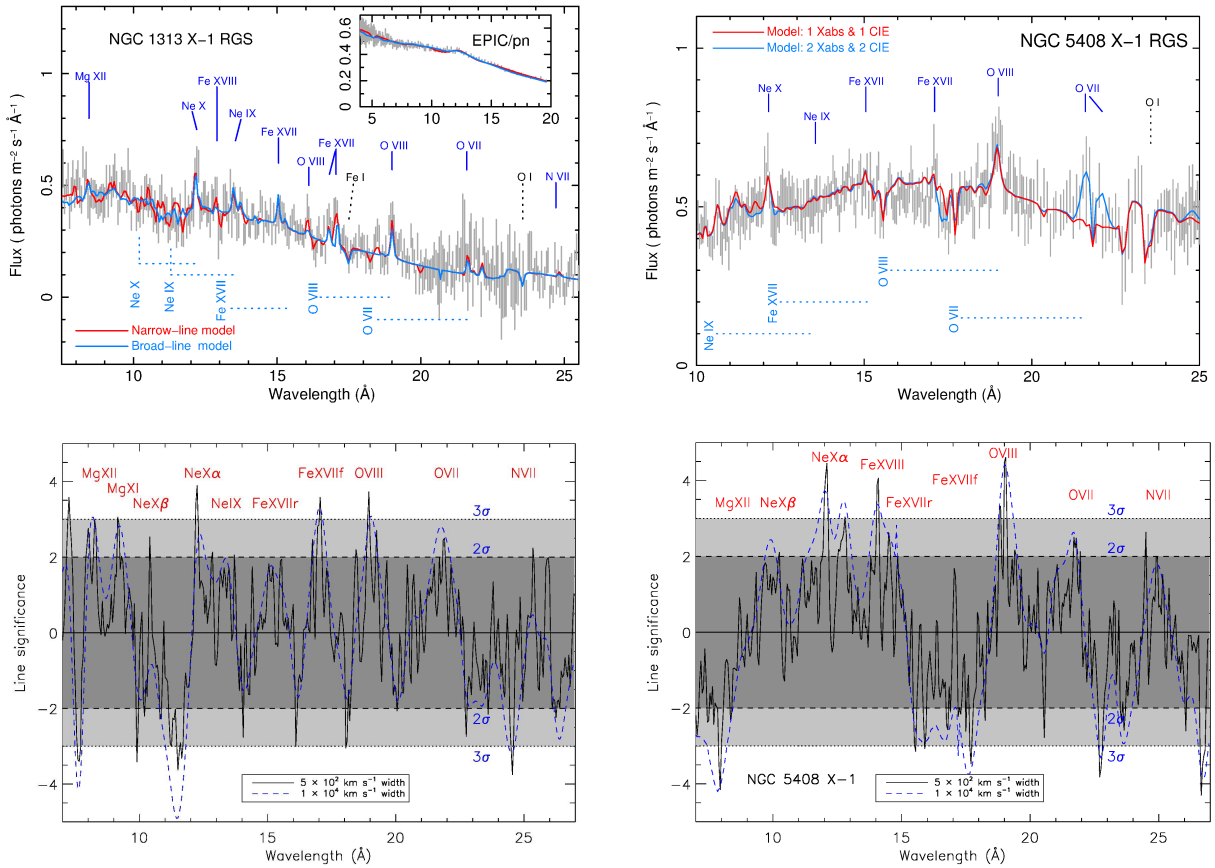

Fig. 3 XMM-Newton/RGS high-resolution grating spectra of NGC 1313 X-1 and NGC 5408 X-1 (top) with overlaid a model of thermal collisionally-ionized emission and a relativistically ($v \sim 0.2c$ blueshifted photoionized absorption. The dotted lines indicate the blueshift from the rest-frame transitions (identical for all absorption lines). Bottom plots show the corresponding line significance obtained by Gaussian fits with increments of 0.05 Å and negative values indicating absorption lines. All plots are from Pinto et al. (2016).

the two ULXs. More detail about the spectral modeling of NGC 1313 X-1 and NGC 5408 X-1 can be found in Pinto et al. (2016).

This is the fastest wind ever detected in a X-ray binary and it could carry enough power to affect its neighbourhood. The outflow rate can be written as $\dot{\mathrm{M}} = 4\pi R^2 \rho v \Omega$, which gives a wind power $P_w = 1/2\,\dot{\mathrm{M}}\,v^2 = 2\pi R^2 m_{\mathrm{p}} n_{\mathrm{H}} v^3 \Omega$, where m_{p} is the proton mass and Ω the solid angle. Since, $\xi = L/n_{\mathrm{H}} R^2$, using the results for the relativistically-broadened absorber, we measure an upper limit for the ratio between the wind power and the luminosity of NGC 1313 X-1 to be $P_w/L = 100\,\Omega\,C_V$. This would imply a highly super-Eddington accretion rate, unless both the covering fraction C_V and the duty cycle are an order of magnitude lower than unity, which is not the case for most ULXs. NGC 1313 X-1, for instance, shows significant spectral features for a large range of spectral hardness (Middleton et al. 2015), which suggests a large covering fraction.

2.5 Fe K powerful ultrafast outflow in NGC 1313 X-1

Motivated by the discovery of a relativistic outflow in these soft X-ray spectra of ULXs, we used the EPIC-pn / MOS 1-2 and FPMA / B longest exposures from XMM-*Newton* and NuSTAR, respectively. These provided total good exposures of 258 ks for EPIC-pn, 331 ks for each EPIC-MOS and 360 ks per FPM (see Walton et al. 2016). We simultaneously fitted these spectra with a cutoff powerlaw (e.g., Stobbart et al. 2006) including neutral absorption both from our Galaxy and intrinsic to NGC 1313.

We searched for Fe K absorption or emission following Walton et al. (2012): we included a narrow (intrinsic width of $\sigma = 10$ eV) Gaussian, and varied its energy across the energy range of interest in steps of 40 eV (oversampling the XMM-Newton energy resolution by a factor $\sim 4-5$). The Gaussian normalisation can be either positive or negative. For each line energy, we record the $\Delta\chi^2$ improvement in fit resulting from the inclusion of the Gaussian line, as well as the best fit equivalent width (EW) and its 90 (1.64σ) and 99% (2.58σ) confidence limits. These are calculated with the EQWIDTH command in XSPEC, using 10,000 param-

© 0000 WILEY-VCH Verlag GmbH & Co. KGaA, Weinheim

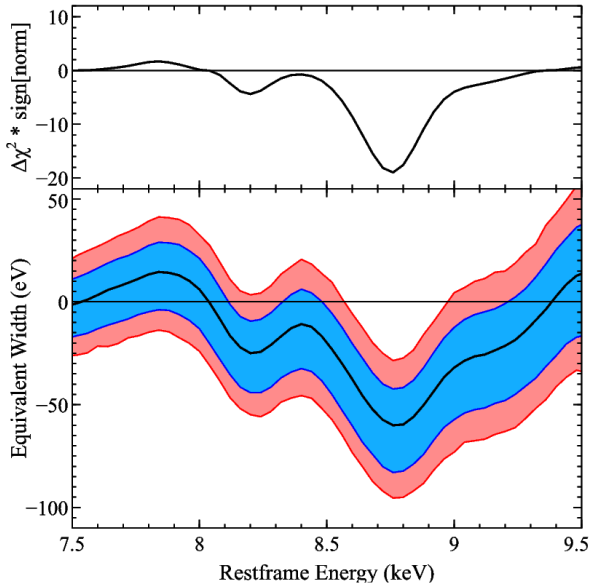

Fig. 4 Detection of Fe K blueshifted absorption (6.70 keV lab energy) in the combined XMM-*Newton* EPIC CCD and NuSTAR FPMA/B CdZnTe spectra. Figure from Walton et al. (2016).

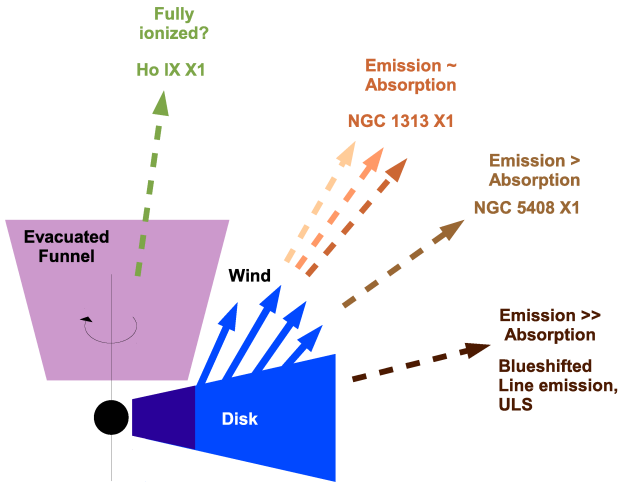

Fig. 5 Cartoon of a physical model of high mass accretion rate sources. The light blue region shows the soft X-ray emission of the accretion disk, altered by a photosphere of a radiatively-driven optically-thick wind. The dark blue region, closer to the compact object is dominated by highly variable, optically-thin, turbulent Comptonization emitting high-energy (> 1 keV) X-rays.

eter simulations based on the best fit model parameters and their uncertainties. To be conservative, we vary the Gaussian line energy between 6.6 and 9.6 keV, corresponding to a wide range of outflow velocities extending up to $> 0.25c$ for Fe XXVI.

The results are shown in Fig. 4 (see also Walton et al. 2016). We detected an absorption line at $8.77\pm^{0.05}_{0.06}$ keV with an equivalent width of -61 ± 24eV, which is comparable to the strongest iron absorption seen from a black hold binary to date (King et al. 2012). We successfully modeled the feature with a photoionized absorber. The best-fit provides ionization parameter $\log \xi = 3.3\pm^{0.3}_{0.5}$, which is higher than that of the gas we detected in the soft X-ray band, but its outflow velocity of $v_{\rm out} = 0.236\pm0.005c$ is in very good agreement with the low-ionization soft X-ray absorber. This fit adopts Fe XXV as dominant ion. Another fit solution with Fe XXVI leading the iron ionic distribution and $v_{\rm out} \sim 0.2c$ is not excluded, but still confirming the presence of a relativistic outflow. We measure a ratio between the wind power and the bolometric luminosity of $P_w/L = 1500\,(60)\,\Omega\,C_V$ for the ionization parameter $\log \xi = 3.3$ (4.5), suggesting that the wind may dominate the energy output from NGC 1313 X-1. Regardless of the precise value of Ω and C_V, these measurements are absolutely extreme if compared to typical sub-Eddington accreting black holes and agree with the predictions for a super-Eddington accretion scenario (e.g., Poutanen et al. 2007; King 2010).

3 Discussion

3.1 XMM-*Newton* – NuSTAR joint efforts

NuSTAR observations have clearly shown that the spectral states of typical ultraluminous X-ray sources present a cut-off above 10 keV, which rules out the interpretation in terms of black holes in a standard low/hard state or reflection-dominated disk regime. Several ULXs, e.g. NGC 1313 X-2, also show spectral transition from states of high luminosity and variability to states of low luminosity without strong variability as expected in transitions from a super-Eddington to a sub-Eddington regime (e.g., Bachetti et al. 2013). The detection of powerful winds in ultraluminous X-ray sources was a missing ingredient for the super-Eddington interpretation of their X-ray luminosities, but our important discoveries of relativistic winds have filled this gap with the theoretical predictions.

3.2 Further insights in super-Eddington accretion

At high accretion rates the disk thickens due to radiation pressure and cools via advection and/or winds; the bolometric luminosity exceeds the Eddington luminosity by a factor proportional to $\log \dot{m}$ (Poutanen et al. 2007). The accretion can increase, orders of magnitude larger than the Eddington limit, where the huge radiation pushes out part of the disk atmosphere at extreme velocities, giving the system a geometry similar to that of a funnel (Fig. 5). The funnel can significantly collimate the X-ray emission via scattering, in which case the disk brightens further (geometrical beaming). The agreement between theory and spectral variability suggests that ULXs are super-Eddington accreting, stellar

© 0000 WILEY-VCH Verlag GmbH & Co. KGaA, Weinheim

mass BHs similar to SS 433, but viewed close to the symmetric axis (e.g., King et al. 2002; Fabrika 2004).

3.3 Wind dependence on the line of sight

In Middleton et al. (2014, 2015) we used the moderate-resolution, but high-sensitivity CCDs on board XMM-*Newton* to show that the absorption features anti-correlate with the spectral hardness. We believe that this trend depends on the viewing angle (see Fig. 5). Close to the symmetric axis the hard X-rays dominate the spectrum smearing out the wind features (Ho IX X-1). At intermediate angles we look directly through the wind and detect strong absorption features, which can vary due to precession (NGC 1313 X-1). At large angles we only see a small portion of the disk; the emission lines, coming from a larger region, are stronger than the absorption lines (NGC 5408 X-1). Edge on, the inner regions are completely obscured by a large amount of cold, optically-thick gas; the source peaks in UV looking like an ultraluminous supersoft X-ray source (Liu et al. 2015). This scenario gives an elegant explanation to the vast phenomenology of ULXs, but needs further evidence with a large sample of ULXs.

3.4 ULXs as cosmological probes

The detection of fully grown SMBHs at high redshifts, and therefore in early stages of the Universe, challenge the theories of the classical sub-Eddington accretion, requiring long periods of higher accretion (see, e.g., Fan et al. 2003, Volonteri et al. 2013). Thorough studies of accretion in high-redshift AGN is beyond the capabilities of the current mission. ULXs are bright, nearby super-Eddington accretors and therefore provide the best means to study the phenomenology of extreme accretors.

3.5 XMM legacy of super-Eddington accretors

Undoubtedly, a statistical sample of typical ULXs is indispensable to confirm the super-Eddington scenario in these sources and to study it in detail. This requires to collect deep gratings and CCD spectra of other ULXs in order to resolve the soft X-ray ubiquitously detected in CCD spectra (see Fig. 1) as well as to probe the highly-ionized Fe K part of the wind. Here we have used NGC 1313 X-1 and NGC 5408 X-1, two archetypal bright ($L_X \sim 10^{40}$ erg/s) ULX, due to their large > 350 ks XMM-*Newton* exposures and we have obtained excellent results, which are encouraging for the future. There are at least a dozen of ULXs with a comparable luminosity and flux that can be thoroughly studied, including those in Fig.1 (Swartz et al. 2004, Liu & Bregman 2005; Walton et al. 2011). We estimated that ~ 2 full XMM-*Newton* orbits per ULX will allow us to resolve the residuals in their EPIC spectra similar to the two ULXs studied here (accounting for solar flares). The gratings on board *Chandra* will also provide an excellent workbench to detect and analyze winds in ULX; in particular they may show some exciting spectral features in the $1.8 - 6$ keV energy band where the XMM-*Newton* instruments lack the require spectral resolution. Due to their lower effective area, the *Chandra* gratings will require exposures of at least 500 ks per ULX.

Acknowledgements. CP and ACF acknowledge support from ERC Advanced Grant 340442. MJM acknowledges support from an STFC Ernest Rutherford fellowship. This paper is based on observations obtained with XMM-*Newton*, an ESA science mission with instruments and contributions directly funded by ESA Member States and the USA (NASA), and NuSTAR, a project led by Caltech, funded by NASA and managed by NASA/JPL.

References

Bachetti, M., Harrison, F., Walton, D.J., et al. 2014, Nature, 514, 202
Bachetti, M., Rana V., Walton D. J., et al., 2013, ApJ, 778, 163
Begelman, M. C. 2002, ApJ, 568, L97
Berghea, C. T., Dudik, R. P., et al. 2010, ApJ, 708, 364
Brinkman, B. C., Gunsing, T., Kaastra, J. S. et al. 2000, SPIE, 4012, 81
Canizares, C. R., Davis, J. E., Dewey, D. et al. 2005, PASP, 117, 1144
den Herder, J. W., Brinkman, A. C., et al. 2001, A&A, 365, 7
Fabrika, S., 2004, ASPRv, 12, 1F
Fan, X., Strauss, M. A., Schneider, D. P., Becker, R. H., White, R. L. et al. 2003, AJ, 125, 1649
Farrell, S. A., Webb, N. A., Barret, D., Godet, O., & Rodrigues, J. M. 2009, Nature, 460, 73
Gladstone, J. C., Roberts, T. P. & Done, C. 2009, MNRAS, 397, 1836
Kaaret, P., Prestwich, A. H., et al. 2001, MNRAS, 321, L29
Kawaguchi, T. 2003, ApJ, 593, 69
King, A. L., Miller J. M., Raymond J., et al., 2012, ApJ, 746, L20
King, A. R., Davies, M. B., Ward, M. J., Fabbiano, G., & Elvis, M. 2001, ApJ, 552, L109
Kormendy, J. & Ho, L. C. 2013, ARA&A, 51, 511
Liu, J.-F., Bai, Yu, Wang, Song 2015, Nature, 528, 108
Liu, J.-F., Bregman, J.N., Bai, Y., Justham, S., & Crowther, P. 2013, Nature, 503, 500
Liu, J.-F. & Bregman, J. N. 2005, ApJS, 157, 59
Long, K. S. & van Speybroeck, L. P. 1983, in Accretion-Driven Stellar X-ray Sources, (Cambridge University Press), p. 117
Middleton, M. J., Walton, D. J., Fabian, A., Roberts, T. P., Heil, L., Pinto, C., Anderson, G., Sutton, A. 2015, MNRAS, 454, 3134
Middleton, M. J., Walton, D. J., Roberts, T. P., Heil, L. 2014, MNRAS, 438, 51
Middleton, M.J., Miller-Jones, J.C.A., et al. 2013, Nature, 493, 187
Miller, J. M., Fabbiano, G., Miller, M. C., & Fabian, A. C. 2003, ApJ, 585, L37
Moon, D.-S., Harrison, F. A., et al. 2011, ApJ, 731, 32
Motch, C., Pakull, M.W., Soria, R., Grisé, F., & Pietrzyński, G. 2014, Nature, 514, 198
Pinto, C., Middleton, M.J., Fabian, A.C. 2016, Nature, 533, 64
Pinto, C., Kaastra, J. S., Costantini, E., de Vries, C. 2013, A&A, 551, 25
Poutanen, J., Lipunova, G., Fabrika, S., Butkevich, A. G., Abolmasov, P. 2007, MNRAS, 377, 1187
Roberts, T.P., Warwick R.S., Ward M.J., Goad M.R., & Jenkins L.P. 2005, MNRAS, 357, 1363

© 0000 WILEY-VCH Verlag GmbH & Co. KGaA, Weinheim

Stobbart, A.-M., Roberts, T.P., & Wilms, J. 2006, MNRAS, 368, 397
Swartz, D. A., Ghosh, K. K., Tennant, A. F., & Wu, K. 2004, ApJS, 154, 519
Volonteri, M., Sikora, M., Lasota, J.-P., Merloni, A. 2013, ApJ, 775, 94
Walton, D.J., Middleton, M.J., Pinto, C., Fabian, A.C., Bachetti, M. 2016, ApJ, 826, 26
Walton, D.J., Harrison, F.A., Greffenstette, B.W., et al. 2014, ApJ, 793, 21
Walton, D. J., Miller J. M., Reis R. C., Fabian A. C., 2012, MNRAS, 426, 473
Walton, D. J., Gladstone, J. C., Roberts, T. P., et al. 2011, MNRAS, 414, 1011

© 0000 WILEY-VCH Verlag GmbH & Co. KGaA, Weinheim